Open access • Journal Article • DOI:10.1002/JEMT.22877

Effects of metals cadmium and chromium alone and in combination on the liver and kidney tissue of male Spraque-Dawley rats: An ultrastructural and electron-energy-loss spectroscopy investigation — Source link

Chantelle Venter, Hester Magdalena Oberholzer, Franscious Cummings, Megan Jean Bester

Institutions: University of Pretoria

Published on: 01 Aug 2017 - Microscopy Research and Technique (Wiley)

Topics: Inner mitochondrial membrane and Endoplasmic reticulum

Effects of metals cadmium and chromium alone and in combination on the liver and kidney tissue of male Spraque-Dawley rats: An ultrastructural and electron-energy-loss spectroscopy investigation

Chantelle Venter[1], Hester Magdalena Oberholzer[1], Franscious Riccardo Cummings[2] and Megan Jean Bester[1]

[1] Department of Anatomy, Faculty of Health Sciences, University of Pretoria, Private Bag x323, Arcadia, 0007, South Africa

[2]Electron Microscope Unit, University of the Western Cape, Private Bag X17, Bellville, 7535, South Africa

Running title: Ultrastructural and EELS analysis of metals

Corresponding Author: H.M. Oberholzer, Department of Anatomy, Faculty of Health Sciences, University of Pretoria, Private Bag x323, Arcadia 0007, South Africa. Tel: +27 (12) 319 2533. Fax: +27 (12) 319 2240. E-mail: nanette.oberholzer@up.ac.za.

Research Highlights

1. Cadmium and chromium causes ultrastructural alterations in the liver and kidney tissue.
2. Cadmium and chromium bio-accumulates in the liver and kidney tissue.
3. Heavy metal exposure may cause functional changes to organs.

Abstract

Heavy metal pollution has increased in the last decades. Water sources are contaminated and human exposure is often long term exposure to variable amounts of different metals. In this study, male Sprague-Dawley rats were exposed via oral gavage for 28 days to cadmium (Cd) and chromium (Cr), alone and in combination at concentrations 1000 times the human World Health Organization`s acceptable water limits. Rat equivalent dosages were used. Blood markers of liver and kidney function were measured, changes to cellular morphology was determined with transmission electron microscopy and the intracellular metal localisation was determined with the electron energy-loss spectroscopy and energy filtered transmission electron microscopy analysis. Both Cd and Cr caused changes to the nuclear

and mitochondrial membranes and irregular chromatin condensation of hepatocytes. Cr exposure caused dilation of the rough endoplasmic reticulum (rER). The combination caused nuclear and mitochondrial membrane damage as well as irregular chromatin condensation. In the kidney tissue, Cd caused irregular chromatin condensation in the cells of the proximal convoluted tubule (PCT). Cr caused changes to the outer nuclear and mitochondrial membrane and chromatin structure. The combination group caused membrane damage, irregular chromatin condensation and rER changes in the PCT. All the metal groups showed damage to the endothelial cells and pedicles, but not to the mesangial cells. Cd and Cr bio-accumulation was observed in the nucleus, mitochondria and rER of the liver and kidney and therefore are responsible for the cellular observed damage that can cause functional changes to the tissues and organs.

Keywords: Heavy metals, environmental toxicity, chronic effects.

Introduction

The growth in the industrial sector has provided many benefits since its establishment, but has come with some unfavourable environmental effects. Heavy metals have become synonymous with industrial pollution due to their toxicological and physiological effects on the ecosystem (Al-Othman and others 2012). Most of the heavy metal pollution can be linked to anthropogenic activities, such as mines, foundries, smelters and other metal-based industrial operations (Al-Attar 2011; Tchounwou and others 2012), with cigarette smoking being the main non-occupational source of heavy metal pollution (Langárd and Costa 2007; Prozialeck and Edwards 2012). The increase in heavy metal levels in the water sources, directly affects the people in the affected areas that are using the water for consumption, preparing food, and bathing, as well as the irrigation of crops. Heavy metals can be absorbed through the skin, orally or through inhalation(Awofolu and others 2005; Venter and others 2015). The degree of heavy metal toxicity depends on dose, duration, route of administration and other physiological factors, especially nutrition (Al-Attar 2011; Chowdhury 2009). In addition, exposure is not limited to a single heavy metal but a mixture of different

types such as a combination of cadmium (Cd), chromium (Cr), Mercury (Hg) and/or Copper (Cu) (Venter and Oberholzer 2015).

In this study the heavy metals Cd and Cr were focused on based on the likelihood of being exposed to them in South Africa. South Africa is known for its thriving mining sector which include manganese, platinum, gold, diamond, chromium and vanadium mines, of which the waste can cause heavy metal pollution, if not discarded correctly. This is unfortunately seen in areas in the Gauteng and Western Cape provinces in South Africa (Malan and others 2015; Venter and others 2015). Both these metals can, depending on the route of exposure, effect the lungs, liver, kidneys, cardiovascular and skeletal systems and may lead to cancer (Jomova and Valko 2011; Langárd and Costa 2007; Prozialeck and Edwards 2012). Only the liver and kidneys were focused on in this study, as these organs play a major role in the absorption, distribution and excretion of toxic compounds, like Cd and Cr (Timbrell 1999). In the liver and kidney, Cd and Cr are metabolized differently, but induce similar effects namely oxidative stress that leads to lipid peroxidation, protein and DNA damage and apoptosis. These effects may lead to functional and ultrastructural changes to the tissue and cellular components of the liver and kidney (Timbrell 1999; Venter and Oberholzer 2015).

The aim of this study was to investigate the possible changes and bio-accumulation in the liver and kidney tissue of male Sprague-Dawley rats after exposure to Cd and Cr alone and in combination.

Material and methods

Spraque-Dawley rat model

Six week old male Spraque-Dawley rats (200-250g) were obtained from the University of Pretoria Biomedical Research Centre (UPBRC). A room temperature of 22°C (±2°C); relative humidity of 50% (±20%) and a 12 hour light/dark cycle were maintained during the entire

study. All experimental protocols complied with the requirements of the University of Pretoria Animal Ethics Committee (Animal ethics number: H009-15). Twenty four rats were randomly divided into four groups, containing 6 rats each. The animals were allowed to acclimatise for 7 days prior to exposure for 28 days.

Metal administration

Cadmium chloride ($CdCl_2$) [Merck (Pty) Ltd, South Africa] and potassium dichromate ($K_2Cr_2O_7$) [Merck (Pty) Ltd, South Africa] were dissolved in sterile water and was administered to the rats via oral gavage. The control rats only received saline and the daily dosages were as indicated in Table 1. Selected concentrations were 1000 times the World Health Organization`s (WHO) acceptable water limits (µg/ℓ) for Cd and Cr (W.H.O. 2011). The metal dosage (µg/ℓ) for an average person of 60.7kg, drinking 1.4ℓ of water per day was calculated and converted using the dose equation of Reagan-Shaw*, et al.* (Bartram and Howard 2003; Reagan-Shaw and others 2008; W.H.O. 2011). The dosages were adjusted weekly according to average weekly weight of the rats. The dosage and duration of exposure represents chronic metal exposure in humans.

Table 1: *In vivo* control and metal dosages

Groups	Dosages	Days
Control	0.5 mℓ Saline	28
Cd	0.854 mg/kg body weight	28
Cr	14.22 mg/kg body weight	28
Cd and Cr	0.854 mg/ kg and 14.22 mg/kg body weight	28

Termination

The rats were terminated via isoflurane overdose, according to standard methods employed by the UPBRC. The liver and kidneys were harvested and processed for transmission electron microscopy (TEM) and electron energy-loss spectroscopy analysis (EELS).

Blood collection

Approximately 5mℓ volume of blood was collected on the day of termination (day 28) via cardiac puncture under isoflurane anaesthesia. The blood was then collected in a citrate tube, and the levels of the following were determined: total serum protein (TP), alanine aminotransferase (ALT), alkaline phosphatase (ALP), aspartate aminotransferase (AST), urea nitrogen (UN), creatinine and total bilirubin (TB).

Statistical analysis

Statistical analysis on the blood chemistry analysis were performed on GraphPad Prism Version 6.01 using 1-way ANOVA and Tukey's multiple comparisons test, where a *p*-value of ≤ 0.05 was considered significant.

Transmission electron microscopy analysis

The liver and kidney tissue samples were cut into $1mm^3$ blocks and fixed in 2.5% glutaraldehyde (GA) and formaldehyde (FA) for 1 hour, rinsed three times in 0.075M sodium potassium phosphate buffer (pH=7.4) for 15 minutes each before the samples were placed in the secondary fixative, a 1% osmium tetroxide solution, for 1 hour. Following fixation, the tissue samples were rinsed again as described above. The tissues were then dehydrated in 30%, 50%, 70%, 90% and three changes of 100% ethanol. The samples were embedded in resin and ultra-thin sections (70-100nm) were cut with a diamond knife using an ultramicrotome. Samples were contrasted with uranyl acetate for 5 minutes followed by 2 minutes of contrasting with lead citrate, after which the samples were allowed to dry for a few minutes before being examined with the JEOL TEM (JEM 2100F).

Electron energy-loss spectroscopy analysis

An FEI Tecnai $G^2$20 high resolution TEM equipped with the GIF 2001 energy filter for EELS and energy filtered transmission electron microscopy (EFTEM) analyses were used to

evaluate the possible bio-accumulation of Cd and Cr in the liver and kidney tissue. EELS spectra [Cd: 403.7eV and Cr: 574eV (Ahn and others 1983)] analysis was done to confirm the presence of the heavy metals in the tissue, together with the EFTEM colour map, to visually express the exact position of the metals in the tissue.

The EELS spectra were collected in normal parallel beam TEM mode, without an objective aperture and employing a GIF entrance aperture of 3mm. This allowed for the use of a large collection semi-angle, β~100mrad, which greatly improved the jump ratio of the spectra. To remove the effects of plural scattering and the contribution from low energy plasmon losses, each spectrum was background subtracted using a power law line shape. This was followed by further deconvoluting the ionization edges using a Log-Fourier iterative process, as to remove all other plural scattering contribution. The EFTEM maps were collected using the Gatan 3 window method with an energy slit width of 20eV. For construction of the Cr map, the pre-edge 1 and pre-edge 2 energy windows were centred at 545 and 565eV, respectively, whereas the post-edge window was centred at 585eV so as to coincide with the onset of the Cr $L_{2,3}$ ionization edge at 574eV. The positions of the pre-edge 1 and 2 windows were based on the background subtraction model obtained from the EELS analyses when using 2 energy windows. This ensured that only energy loss contributions from the metal under investigation were mapped. Similarly, for mapping of the energy-loss contributions of Cd, the pre-edge 1 and 2 windows were placed at 364 and 384eV, with a post-edge onset centred at 414eV.

Results

In a rat model representing chronic oral exposure to Cd and Cr alone and in combination at 1000 times the WHO limit the effects of exposure on blood parameters and tissue ultrastructure was evaluated.

Table 2: Organ specific blood chemistry analysis

	TP (g/ℓ)		UN (mmol/ℓ)		Creatinine (µmol/ℓ)	
	Range	**Mean ± SD**	**Range**	**Mean± SD**	**Range**	**Mean ± SD**
Control	53.9 - 62.7	58.30 ± 3.65	7.0 – 8.0	7.55 ± 0.41	24 - 30	27.17 ± 2.23
Cd	58.3 - 61.6	60.18 ± 1.29	5.9 - 7.9	7.03 ± 0.78	23 - 26	24.17 ± 1.17
Cr	54.2 - 58.5	56.28 ± 1.63	6.0 - 9.1	7.68 ± 1.05	22 - 28	25.33 ± 2.34
Cd & Cr	52.0 - 61.3	54.30** ± 3.54	6.4 - 7.6	6.95 ± 0.42	21 - 25	23.17* ± 1.83
	ALT (U/ℓ)		**ALP (U/ℓ)**		**AST (U/ℓ)**	
	Range	**Mean ± SD**	**Range**	**Mean± SD**	**Range**	**Mean ± SD**
Control	55 - 69	61.50 ± 5.58	163 - 245	201.67 ± 30.43	82 - 140	94.67 ± 24.90
Cd	50 - 66	57.17 ± 6.37	156 - 198	183.33 ± 14.79	73 - 80	77.60 ± 2.88
Cr	42 - 64	56.33 ± 9.03	121 - 223	165.33 ± 38.47	79 - 245	130.17 ± 58.54
Cd & Cr	52 - 65	57.67 ± 5.50	122 - 165	146.33* ± 18.45	75 - 138	110.67± 26.69

	TB (µmol/ℓ)	
	Range	**Mean ± SD**
Control	0.3 – 1.1	0.70 ± 0.30
Cd	0.6 – 1.4	0.93 ± 0.28
Cr	0.7 – 1.6	0.97 ± 0.33
Cd & Cr	0.7 – 1.3	1.02 ± 0.21

*statistical significance compared to control, ** statistical significance compared to Cd: *p*-value of ≤0.05. SD: Standard deviation

Blood chemistry test

The TP levels in the combination group were significantly lower than that of the group exposed to Cd alone. The levels of ALP and creatinine in the combination group were significantly lower than the control group. The bilirubin levels, although not statistically significant, showed a slight increase in the exposed groups, compared to the control. Compared to the controls no increases in ALT, AP or AST were observed (Table 2).

Transmission electron microscopy

With TEM, the following ultrastructural features associated with tissue damage were sought and this included cellular, nuclear and mitochondrial membrane disruption, irregular chromatin condensation, mitochondrial inner membrane swelling and rough endoplasmic reticulum (rER) dilation. For the kidney this included the ultrastructural of the endothelial cells, pedicles, podocytes and mesangial cells.

In Figure 1 the hepatocytes and nuclear ultrastructure of these cells are presented. Normal hepatocyte morphology was observed in all control samples (Fig. 1A). Only minimal alterations to the nuclear [Fig. 1B (arrow)] and mitochondrial membranes [Fig. 2B (arrow)], were observed in all the rats. No inner matrix alterations were seen in the mitochondria of the control liver tissue (Fig. 2A). The hepatocytes of the Cd exposed group showed the presence of nuclear and mitochondrial membrane disruptions that were more prevalent than in the control group [Fig. 1D (arrow) and 2D, respectively]. Irregular chromatin condensation is present in the nuclei (Fig. 1C), but no inner matrix swelling is seen in the mitochondria (Fig. 2C). In the Cr experimental group, nuclear outer membrane [Fig. 1F (arrows)] and mitochondrial membrane alterations were visible (Fig. 2F), accompanied by irregular chromatin condensation in the nuclei (Fig. 1E) and inner matrix swelling present in the cristae of the mitochondria [Fig. 2E (arrow)]. There was also a noteworthy increase in the dilation of the rER [Fig. 1E (arrows)]. In the combination group an increase in both nuclear membrane [Fig.1H (arrows)] and chromatin condensation alterations were noted (Fig. 1G). The metal combination group also revealed changes to the mitochondrial membranes and cristae [Fig. 2G and H (arrows)].

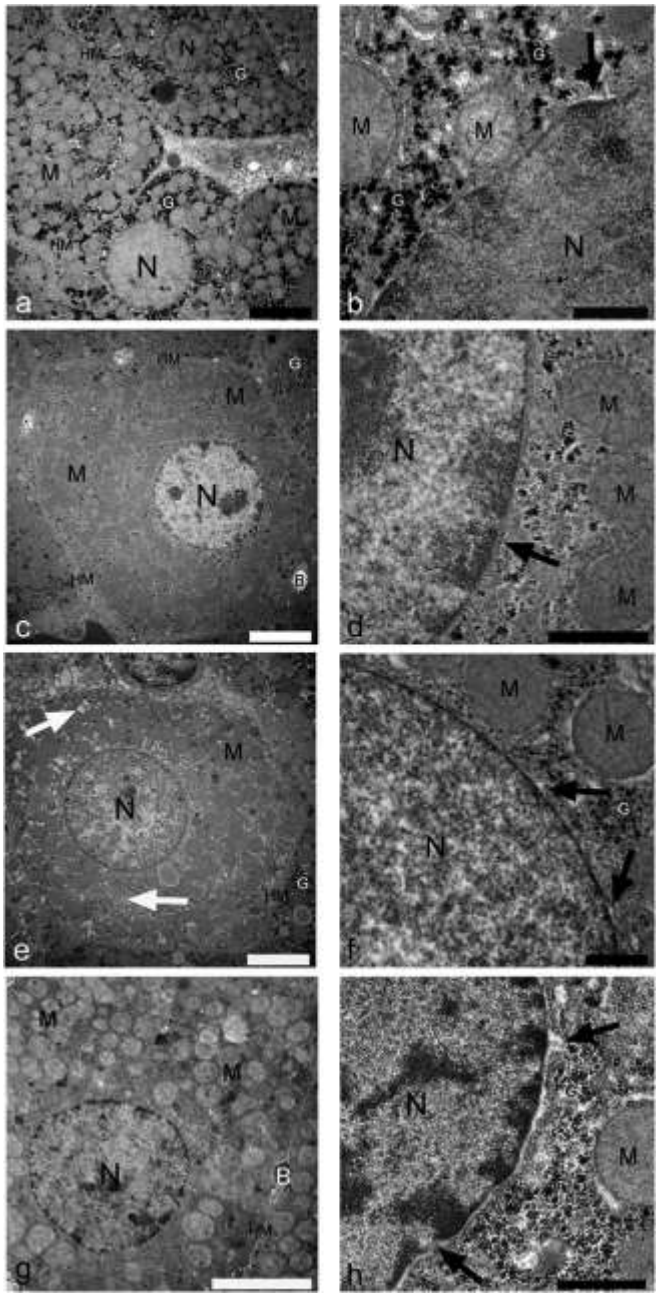

Figure 1: TEM micrographs of the hepatocytes of the liver tissue in the control (A and B), Cd (C and D), Cr (E and F) and Cd and Cr (G and H) groups. Black arrows indicate membrane alterations and white arrows indicate rER dilation. **Key:** G: Glycogen granules; M: Mitochondria; N: Nucleus (Scale bars: A, C, E, G: 5µm; B, D, F, H: 1µm).

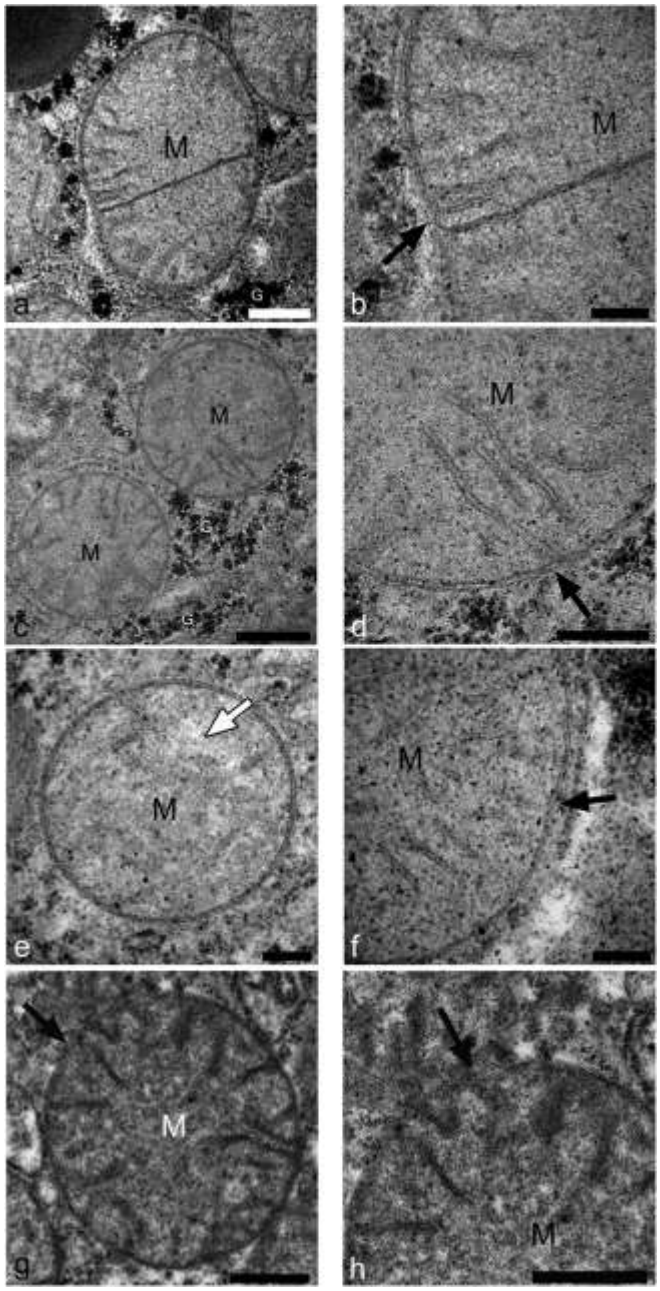

Figure 2: TEM micrographs of the mitochondria of the liver tissue of the control (A and B), Cd (C and D), Cr (E and F) and Cd and Cr (G and H) groups. Black arrows indicate membrane alterations, with the white arrow that indicates inner matrix swelling. **Key:** G: Glycogen granules; M: Mitochondria; N: Nucleus (Scale bars: A, C, G, H: 500nm; B, D, E, F: 200nm).

The two main areas of the kidney involved in toxicity and filtration were evaluated. Firstly the proximal convoluted tubule (PCT) was analysed, as it is the part of the kidney most likely to show any changes that occurred in the kidney tubules (Tavafi, *et al.*, 2016). The second area of the kidney analysed was the glomeruli. The glomeruli will show any changes in the

filtration system of the kidney. In the control group, minimal changes were seen in a few of the rats analysed, with negligible nuclear outer membrane alterations [Fig. 3C (arrow)] as well as mitochondrial membrane changes (Fig. 3E). No changes were seen in the PCT cell membrane, rER (Fig. 3A) and mitochondrial cristae (Fig. 3E) as would be expected for the control samples. The components of the glomeruli: endothelial cells (involved in the filtration system), pedicles, mesangial cells and podocytes, all showed minimal to no alterations in the control group (Fig. 3B, D and F). Changes in the organelles of the PCT of the Cd exposed group (Fig. 4C and E) were more prevalent than in the control group, with a noteworthy increase in the occurrence of irregular chromatin condensation seen in the nucleus (Fig. 4A). Minimal alterations were also seen in the endothelial cells and pedicles of the glomeruli [Fig. 4B and D (arrow)]. No changes were noted in the mesangial cells and podocytes (Fig. 4F).

In the Cr experimental group, changes were seen in the outer membrane [Fig. 5 C (arrows)] and chromatin of the nucleus (Fig. 5A), as well as in the mitochondrial membranes [Fig. 5E (black arrow)]. Minimal alterations were visible in the PCT cell membrane, rER (Fig. 5A) and mitochondrial cristae [Fig. 5E (white arrow)] in almost all the animals in this group. The endothelial cells [Fig. 5D (white arrows)] and pedicles [Fig 3B and D (black arrows)] showed minimal damage in almost all the rats, with no changes seen in the mesangial cells (Fig. 5F) and podocytes. The kidney tissue of the combination of Cd and Cr group also showed changes in the nucleus and mitochondria, with membrane alterations [Fig. 6C and E (black arrows)] and irregular chromatin condensation (Fig. 6A) and inner matrix swelling [Fig. 6E (white arrow)]. Some cellular membrane and rER changes were also seen in the PCT (Fig. 6A). The endothelial cells and pedicles also showed alterations in almost all the experimental rats [Fig. 6B (arrow) and D], with no changes seen in the mesangial cells (Fig.6F).

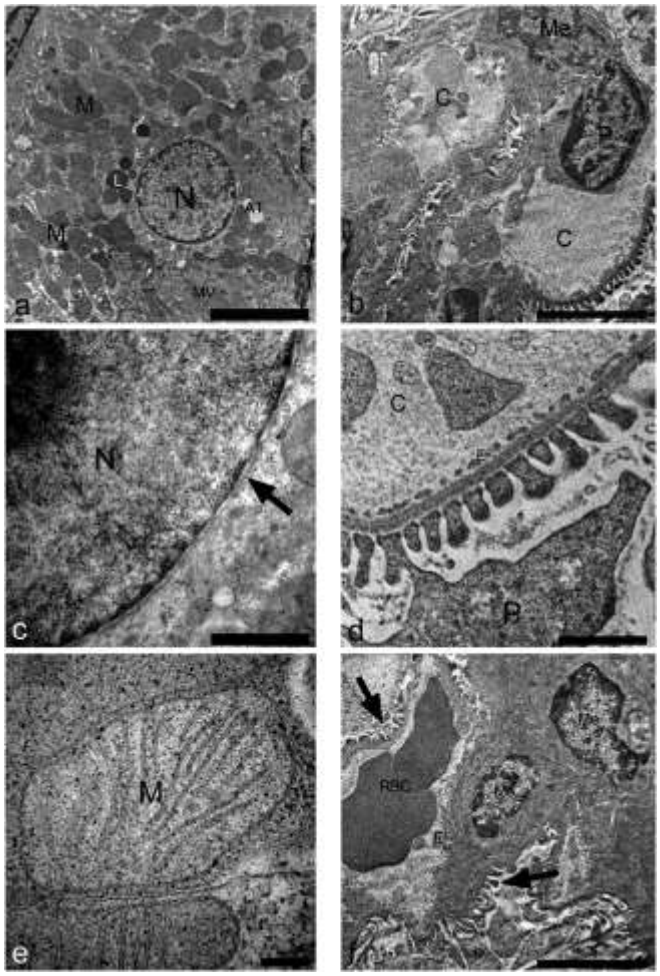

Figure 3: TEM micrographs of the kidney tissue of the control group. Figure A, C and E indicate the PCT, nuclear membrane and mitochondria, respectively. The glomeruli ultrastructure can be seen in Figure B, D and F. **Key:** AT: Apical tubulovesicles C: Capillary; E: Endothelial cell; L: Lysosome; Me: Mesangial cell; MV: Microvilli; M: Mitochondria; N: Nucleus; P: Podocyte; RBC: Red blood cell (Scale bars: A, B and F: 5µm; C and D: 1µm; E: 500nm).

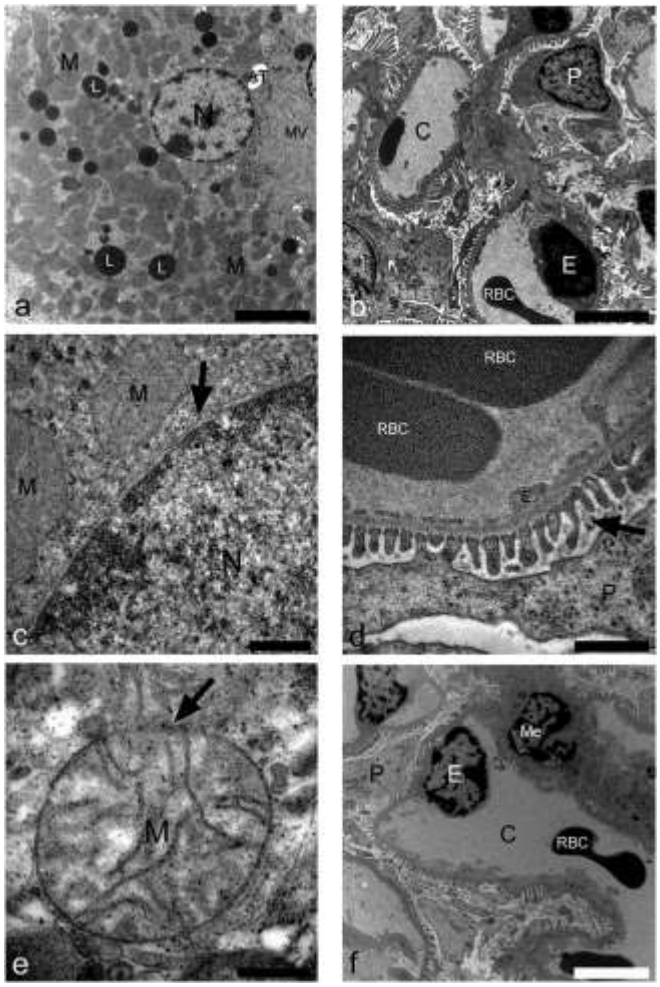

Figure 4: TEM micrographs of the kidney tissue of the Cd experimental group. Figure A, C and E indicate the PCT cuboidal epithelial cell, nucleus and mitochondria, respectively, with the arrows indicating membrane changes. Figure B, D and F shows the glomeruli and all its components, with the arrow in Figure D indicating the pedicles. **Key:** AT: Apical tubulovesicles; C: Capillary; E: Endothelial cell; L: Lysosome; Me: Mesangial cell; MV: Microvilli; M: Mitochondria; N: Nucleus; P: Podocyte; RBC: Red blood cell (Scale bars: A, B and F: 5µm; C and D: 1µm; E: 500nm).

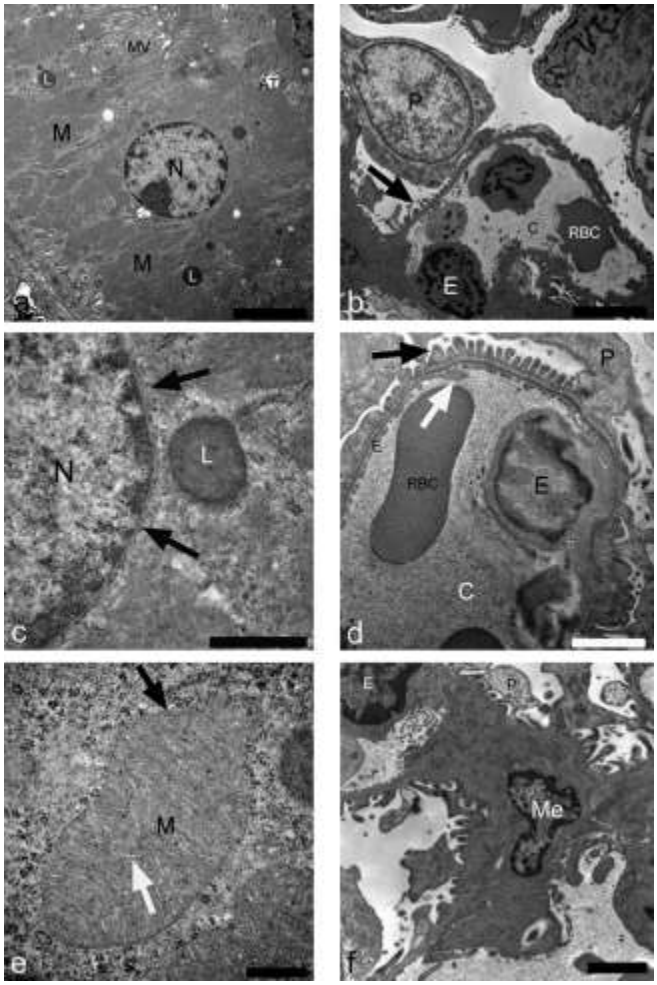

Figure 5: TEM micrographs of the kidney tissue of the Cr group. Figures A, C and E represents the alterations seen in the PCT cells, with Figure C (arrows) indicating changes in the outer membrane of the nucleus and Figure E shows changes in the membrane (black arrow) and cristae (white arrow). Figures B, D and F show the glomeruli, where endothelial cells, podocytes and mesangial cells alterations are shown. In Figure B and D the black arrows show damage to the pedicels and the white arrow (Fig. D) indicates endothelial cell damage. **Key:** AT: Apical tubulovesicles; C: Capillary; E: Endothelial cell; L: Lysosome; Me: Mesangial cell; MV: Microvilli; M: Mitochondria; N: Nucleus; P: Podocyte; RBC: Red blood cell (Scale bars: A, B and F: 5µm; C and D: 1µm; E: 500nm).

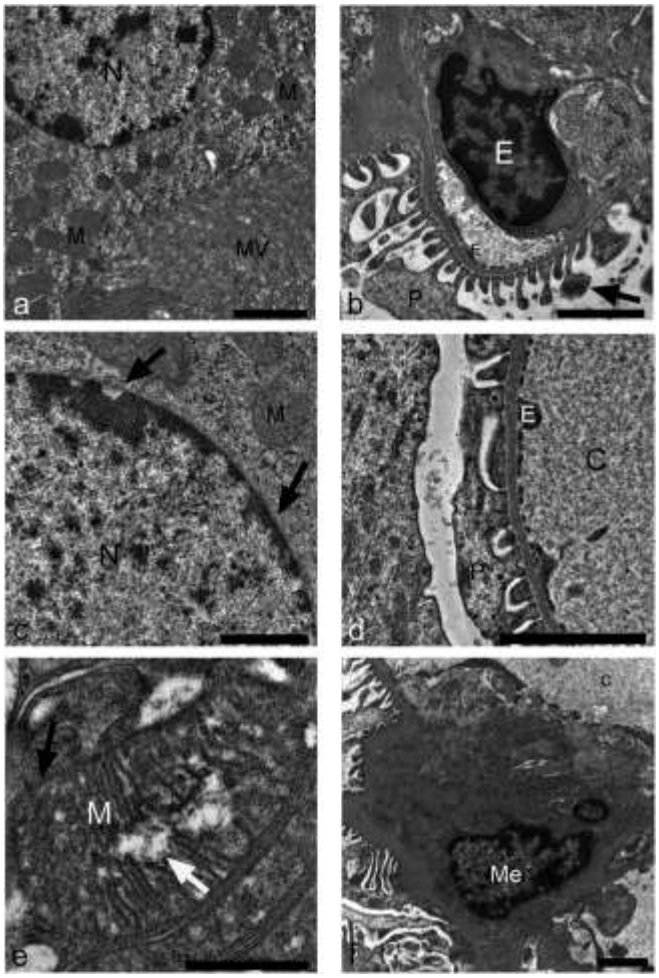

Figure 6*:* TEM micrographs of kidney tissue of the Cd and Cr group. Figure A indicates the PCT, with Figures C and E showing the alterations seen in the nucleus and mitochondria (arrows), respectively. Figures B, D and F show the glomeruli and components. **Key:** C: Capillary; E: Endothelial cell; Me: Mesangial cell; MV: Microvilli; M: Mitochondria; N: Nucleus; P: Podocyte (Scale bars: A, B, D and F: 2µm; C and E: 1µm).

Electron energy-loss spectroscopy

The following figures are examples of how the EELS and EFTEM results were generated when analysing the liver and kidney samples of all the experimental groups.

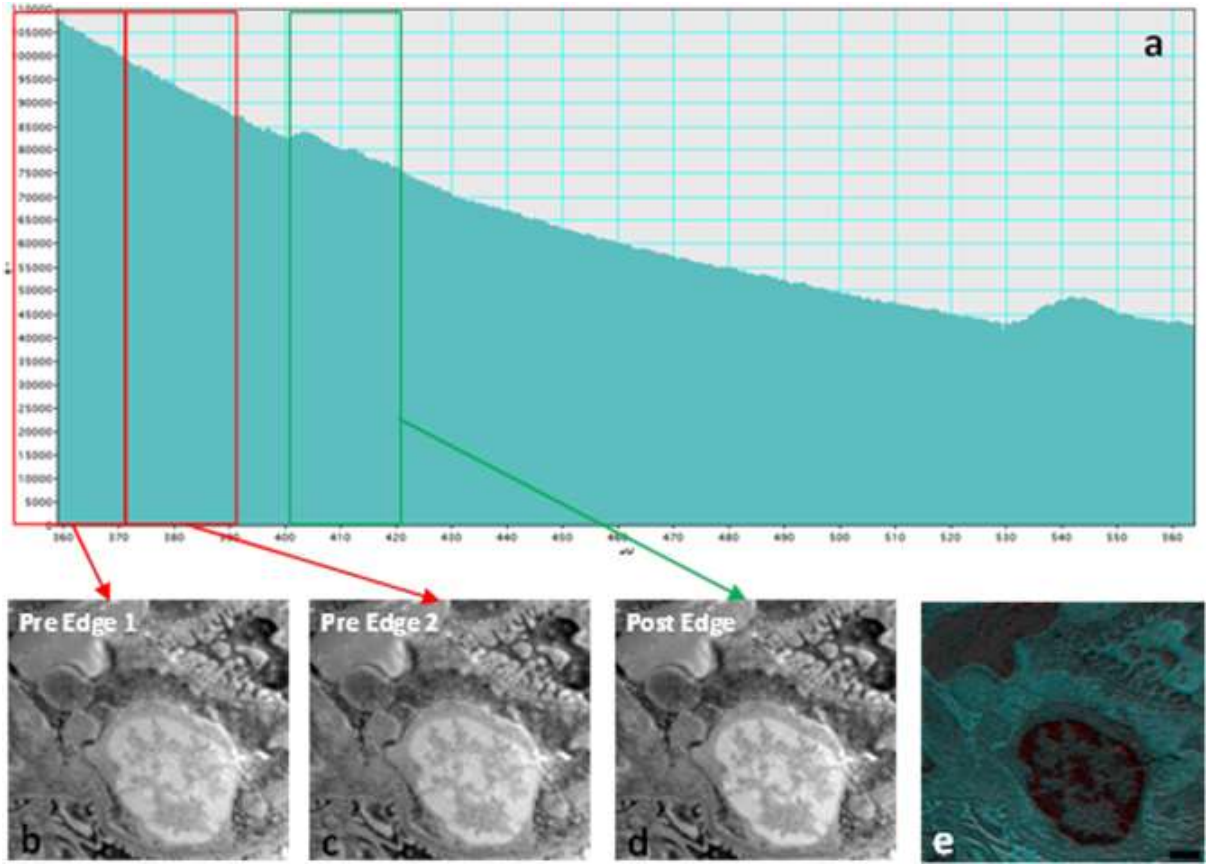

Figure 7: EELS and EFTEM micrographs of Cd exposed kidney tissue. Figure A shows the Cd edge that was used in the EELS analysis, with Figures B-D indicating the pre- and post-edge micrographs of Cd in the glomeruli of the kidney at each specific edge that was analysed. Figure E indicates the final Cd map, with the Cd in red (Scale bars: B, C, D and E: 1µm).

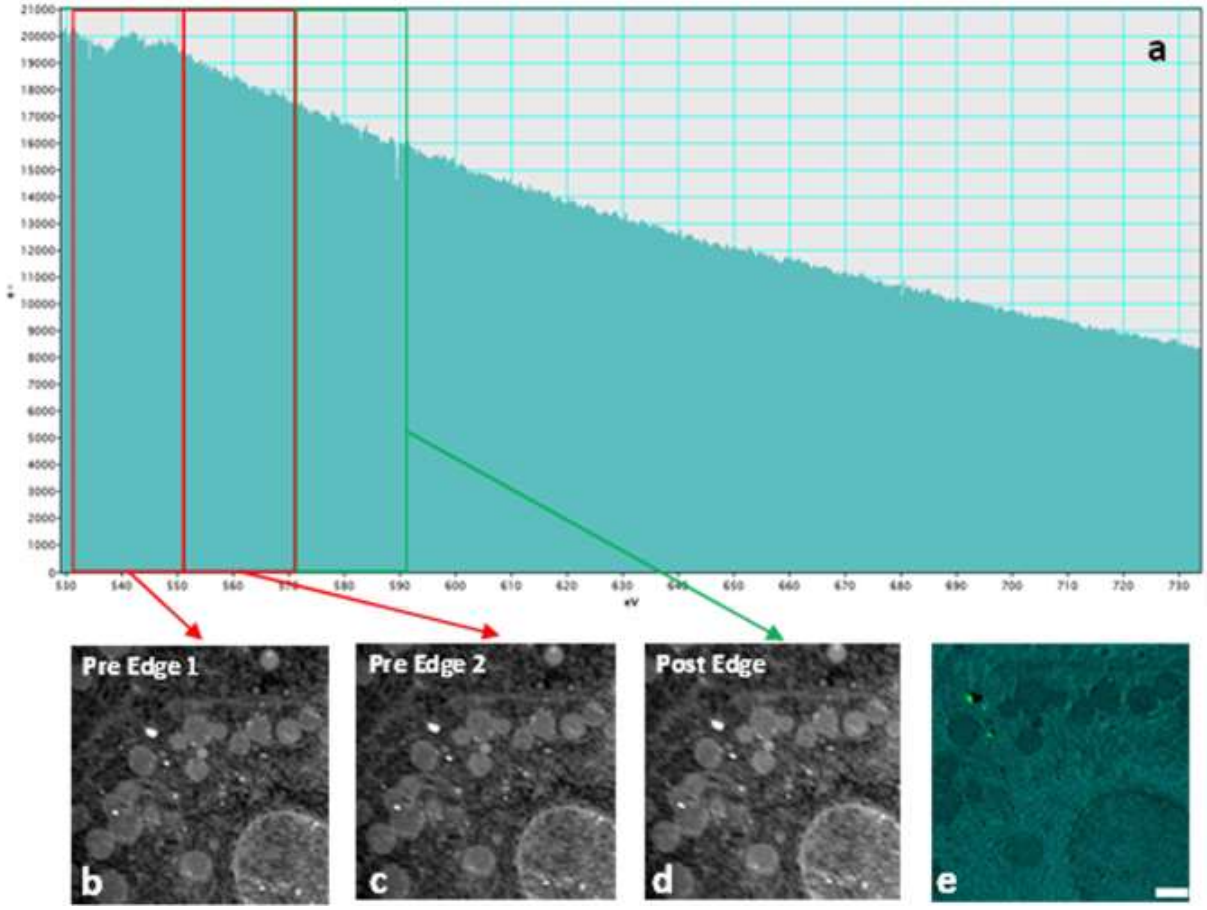

Figure 8: EELS and EFTEM micrographs of Cr exposed liver tissue. Figure A shows the Cr edge that was used in the EELS analysis, with Figures B-D indicating the pre- and post-edge micrographs of C of the liver at each specific edge that was analysed. Figure E indicates the final Cr map, with the Cr in yellow (Scale bars: B, C, D and E: 1µm).

Energy filtered transmission electron microscopy

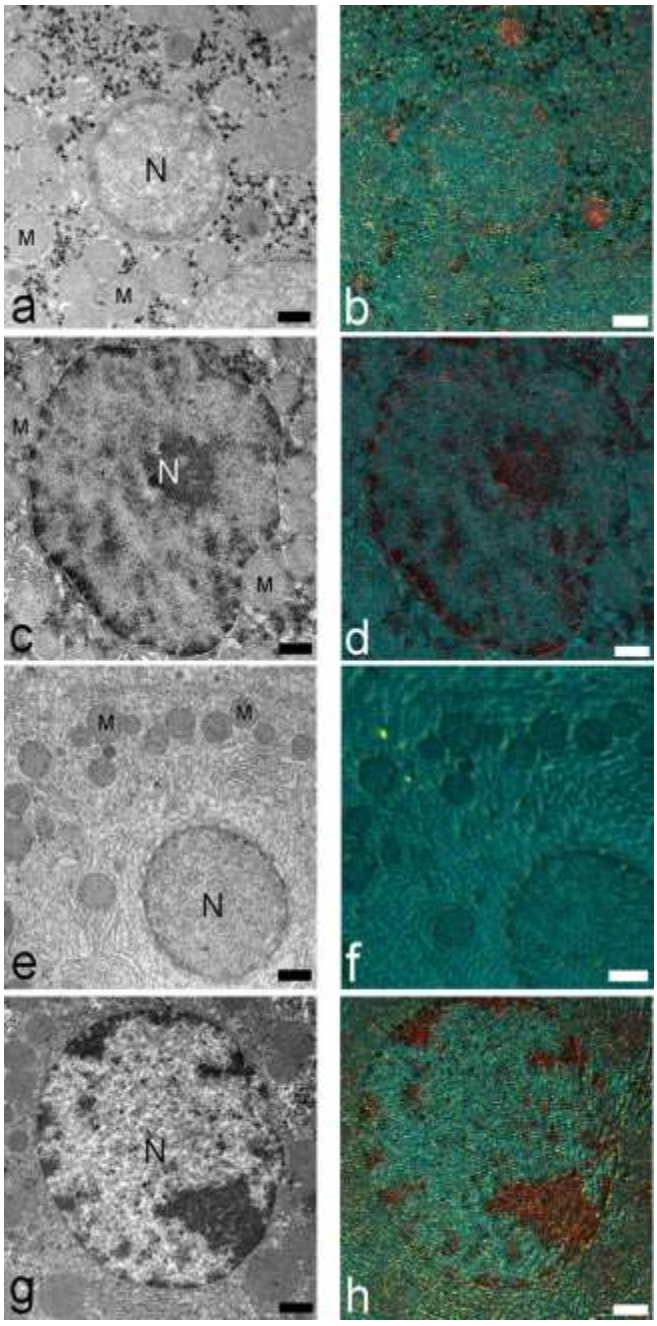

Figure 9: EFTEM micrographs of the liver tissue of the control (A and B), Cd (C and D), Cr (E and F) and Cd and Cr (G and H). Figure A, C, E and G indicates the zero loss images of the colour maps in Figure B, D, E and H, with Cd in red and Cr in yellow. **Key:** N: Nucleus; M: Mitochondria (Scale Bars: A-H: 1µm).

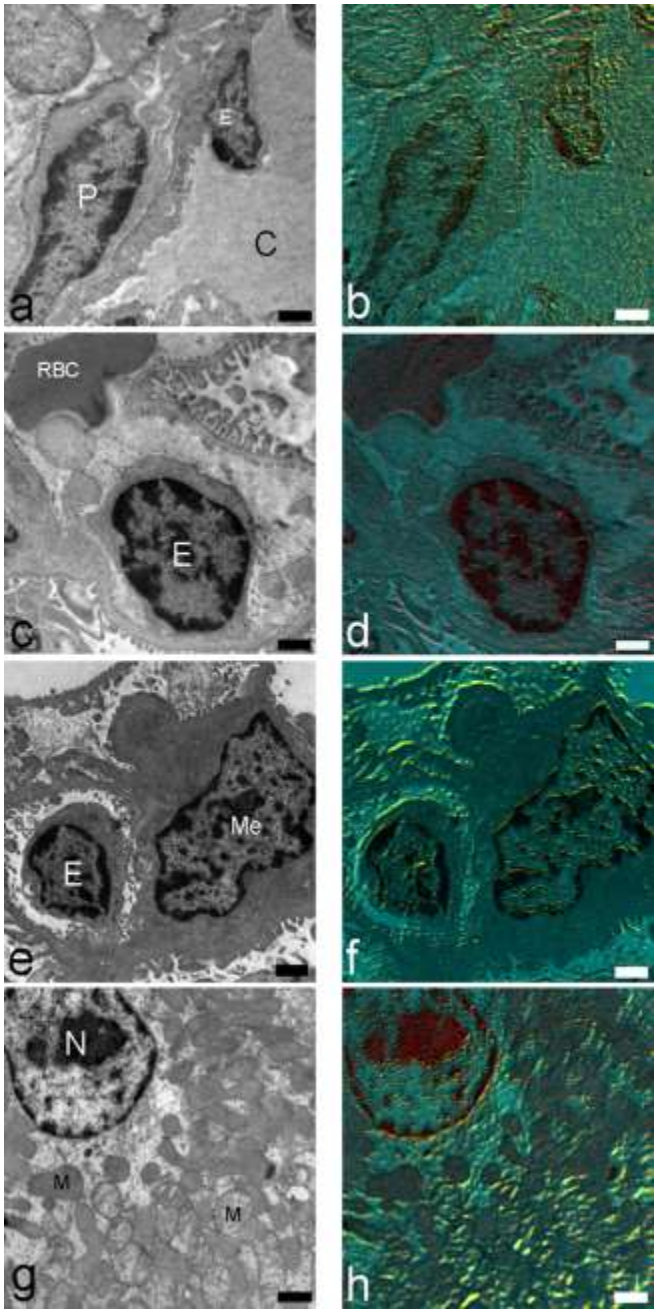

Figure 10: EFTEM micrographs of the kidney tissue of the control (A and B), Cd (C and D), Cr (E and F) and Cd and Cr (G and H). Figure A, C, E and G indicates the zero loss images of the colour maps in Figure B, D, E and H, with Cd in red and Cr in yellow. **Key:** N: Nucleus; M: Mitochondria; C: Capillary; E: Endothelial cell; P: Podocyte; RBC: Red blood cell (Scale Bars: A-H: 1µm).

Further evaluation of the tissue with EELS and EFTEM, identified that Cd and Cr bio-accumulates in the liver and kidney, as can be seen in Figures 9 and 10, even though only minimal energy-loss signals were obtained in both the Cd and Cr groups, alone and in combination.

Figures 7 and 8 A show examples of the Cd and Cr edges that were used in the EELS analysis, respectively, where Figures 7 and 8 B-D show the Cd and Cr in the organelles of the kidney and liver, respectively, at each specific edge that was analysed, with the final Cd and Cr colour map seen in Figures 7 and 8 E, with Cd in red and Cr in yellow.

In Figure 9 and 10 the EFTEM micrographs are shown of the liver and kidney tissue, respectively. The analysis of the control group showed a noisy signal that does not bio-accumulate specifically in any organelle (Fig. 9 and 10 A and B). With the Cd exposed groups, the EFTEM analysis revealed that Cd bio-accumulates not only in the organelles, but also on the membranes of the organelles (Fig. 9 and 10 C and D, respectively). Cr on the other hand mostly bio-accumulates on the membranes of the organelles (Fig. 9 and 10 E and F). This trend of specific localisation was also seen in the Cd and Cr group with EFTEM analysis (Fig. 9 and 10 G and H).

Discussion

The increase in heavy metal exposure is of great concern and the effects on the environment, animals and humans should be constantly evaluated (Al-Attar 2011). Heavy metals, such as Cd and Cr, have the potential to alter cellular functions by catalysing the formation of radicals, inhibition of antioxidant enzymes and binding to antioxidant elements such as glutathione (GSH) this leads to oxidative stress. This results in increased lipid peroxidation, protein and DNA damage and apoptosis, that can lead to associated diseases such as hepatic necroinflammation, non-alcoholic steatohepatitis, fibroplasias, renal fibrosis and failure, and cancer (Bertin and Averbeck 2006; García-Niño and Pedraza-Chaverrí 2014; Jin and others 2014; Khlifi and others 2013; Sarkar and others 2013; Thévenod and Lee 2015; Timbrell 1999; Venter and Oberholzer 2015).

Many studies have investigated the effect of Cd or Cr administered either as a single dosage or as several smaller dosages over a period of several days. Although these studies identify the toxicity of these metals, the relevance of dosage related to actual human exposure is unknown. In the present study, metal dosages were selected to identify the effect of a 1000 times human exposure limit on liver and kidney function and structure using a rat model. Very rarely is exposure to a single metal but rather complex mixtures of metals in varying concentrations and therefore this is a first of a series of studies we wish to undertake to evaluate the toxicity of metal combinations.

Blood markers of liver and kidney damage were not raised, indicating normal liver and kidney function. TP, ALP and creatinine levels were reduced but were only significant for the Cd and Cr combination group compared to the control. A reduction in ALP levels have been reported for rats treated with $CdCl_2$ (El-Demerdash and others 2001; El-Demerdash and others 2004; Rana and others 1996). Cd can influence zinc either through replacing membrane associated zinc or inhibiting apoptosis and necrosis prevention properties of zinc (El-Demerdash and others 2004; Jacquillet and others 2006). Zinc is a cofactor essential for ALP function and with zinc displacement ALP synthesis and function is compromised (Suzuki and others 2005). Compared to the control, creatinine levels were significantly lower in the metal combination group and may indicate renal tubular dysfunction (Asagba and Obi 2004; Babaknejad and others 2015). Several researchers have also reported lower ALP and creatinine levels after exposed to Cr (Kumar and Kumar 2013; Kumar and others 1984). The TP and bilirubin levels (although the latter was not significant) were altered and may suggest early changes in liver and kidney function. Similar results were obtained in the studies of Lakshimi, *et al*. and Kumar, *et al*. where after exposure to Cd and Cr, the TP and bilirubin levels were decreased and increased respectively (Kumar and others 2013; Lakshmi and others 2012). The blood chemistry results show no major damage to the liver or kidneys. However, small reductions in TP, creatinine and ALP indicates that some changes in the tissue biochemical functioning has occurred.

The morphological changes and bio-accumulation of Cd and Cr alone and in combination in the liver and kidneys of male Sprague-Dawley rats was then analysed. Minor ultrastructural changes were found in nucleus, mitochondria and rER of all the experimental groups. Organ specific changes were also seen in the components of the glomerular filtration barrier namely the pedicles and endothelial cells. Small amounts of the metals were found in the liver and kidney tissue with the EELS and EFTEM analysis. The Cd accumulated in the nucleus and mitochondria, where Cr was primarily found at the membranes of the nucleus, mitochondria and rER.

Reactive oxygen species (ROS) is generated in several organelles including the endoplasmic reticulum and mitochondria. This occurs during normal cellular metabolism such as oxidative protein folding and mitochondrial respiration and this process is tightly regulated. ROS levels are regulated by the presence of antioxidant enzymes such as catalase, superoxide dismutase and glutathione peroxidase as well as antioxidant elements such as GSH and dietary antioxidants such as vitamins E and C. Cd and Cr toxicity affects certain components of the cellular antioxidant system and when in combination these effects are accumulative.

Cd does not catalyse the Fenton reaction but binds intracellular thiols, like GSH and/or inhibits the activity of antioxidant enzymes such as catalase (Prozialeck and Edwards 2012). Consequently levels of hydrogen peroxide (H_2O_2), superoxide anion (O_2•) and hydroxyl radical (•OH) are increased (Bertin and Averbeck 2006; Jomova and Valko 2011). These ROS cause lipid membrane peroxidation as well as protein and DNA damage. A consequence of protein damage and lipid peroxidation are changes in membrane function and stability (Bertin and Averbeck 2006). This is associated with changes in the morphology of membranous organelles such as the mitochondria as well as plasma and nuclear membranes. Cd was found to accumulate in the mitochondria and nuclei and in these intracellular compartments, Cd can bind membrane and DNA associated proteins thereby

altering membrane integrity and function as well as DNA repair mechanisms (Bertin and Averbeck 2006). This in turn can lead to cell cycle arrest, apoptosis, genome instability, mutagenesis eventually leading to cancer.

The biochemical pathway of Cr firstly involves the reduction of hexavalent Cr [Cr(VI)] to less toxic trivalent Cr [Cr(III)]. This is mediated by antioxidant elements like ascorbate, one of the most effective biological reductant of Cr(VI), and non-enzymatic reactions with cysteine and GSH. This reduction of Cr(VI) to Cr(III) comes with a price as it generates high levels of Cr-DNA adducts and mutations that leads to DNA damage (Jomova and Valko 2011). This would affect the structure and function of both genomic and mitochondrial DNA. In addition a tightly regulated process of ROS formation occurs in the mitochondria and the endoplasmic reticulum. The accumulation of Cr which is catalyst of the Fenton reaction with cause ROS homeostasis to be disrupted, resulting in increased lipid membrane peroxidation, altered protein processing eventually leading to apoptosis. Cr toxicity also affects the mitogen-activated protein kinases (MAPK) signal transduction pathway, where nuclear factor kappa B (NF-κB), activating transcription factor 2 (ATF-2) and p53 plays a role in regulating cellular processes, including apoptosis (Jomova and Valko 2011).

In a previous *in ovo* study by the authors, we found that increasing concentrations of Cd and Cr caused increased organelle damage associated with the accumulation of Cd and Cr in the nuclei and mitochondria of the liver and kidney (Venter and Oberholzer 2015). Madejczyk, *et al.*, undertook a time based study and found that with a single intraperitoneal injection there was accumulation of Cd and Cr in the liver. With time metal levels decreased but ROS and cellular damage increased. This was associated with changes in the expression of genes associated with oxidative stress, metabolism, DNA damage, cell cycle and inflammatory responses (Madejczyk and others 2015). The present study clearly shows that Cd and Cr accumulate in specific compartments such as the mitochondria, rER, nucleus and membranes directly involved with these processes.

Conclusion

In conclusion, exposure to Cd and Cr alone and in combination at levels that do not increase markers of liver or kidney damage however these metals were found to cause changes in the ultrastructure of several organelles of the liver and kidney. Metal bio-accumulation was observed in the nucleus, mitochondria and rER of the liver and kidney. At these sites the metals can induce DNA- and protein damage and lipid peroxidation which can cause functional changes in tissue and organ function.

Acknowledgements

The authors would like to thank the National Research Foundation for their financial support and Dr James Wesley-Smith of the Council for Scientific and Industrial Research National Centre for nano-structured materials for the use of their TEM.

References

Ahn, C., Krivanek, O., Burgner, R., Disko, M., & Swann, P. (1983). EELS Atlas Gatan Inc. *Warrendale, PA*, 1-93.

Al-Attar, A.M. (2011). Antioxidant effect of vitamin E treatment on some heavy metals-induced renal and testicular injuries in male mice. *Saudi Journal of Biological Sciences,* 18(1), 63-72.

Al-Othman, Z.A., Ali, R., & Naushad, M. (2012). Hexavalent chromium removal from aqueous medium by activated carbon prepared from peanut shell: adsorption kinetics, equilibrium and thermodynamic studies. *Chemical Engineering Journal,* 184, 238-247.

Asagba, S., & Obi, F. (2004). Effects of oral cadmium exposure on renal glomerular and tubular functions in the rat. *Journal of Applied Sciences and Environmental Management,* 8(1), 29-32.

Awofolu, O., Mbolekwa, Z., Mtshemla, V., & Fatoki, O. (2005). Levels of trace metals in water and sediment from Tyume River and its effects on an irrigated farmland. *Water Sa,* 31(1), 87-94.

Babaknejad, N., Moshtaghie, A.A., Shahanipour, K., & Bahrami, S. (2015). Protective Effects of Magnesium on Cadmium Renal Toxicity in Male Wistar Rats. *Zahedan Journal of Research in Medical Sciences*, 29-32.

Bartram, H.G., & Howard, G. (2003). Domestic water quantity: Service level and health. *Geneva: World Health Organization*.

Bertin, G., & Averbeck, D. (2006). Cadmium: cellular effects, modifications of biomolecules, modulation of DNA repair and genotoxic consequences (a review). *Biochimie,* 88(11), 1549-1559.

Chowdhury, A.R. (2009). Recent advances in heavy metals induced effect on male reproductive function-A retrospective. *Al Ameen Journal of Medical Sciences,* 2(2), 37-42.

El-Demerdash, F., Yousef, M., & Elagamy, E. (2001). Influence of paraquat, glyphosate, and cadmium on the activity of some serum enzymes and protein electrophoretic behavior (*in vitro*). *Journal of Environmental Science and Health, Part B,* 36(1), 29-42.

El-Demerdash, F.M., Yousef, M.I., Kedwany, F.S., & Baghdadi, H.H. (2004). Cadmium-induced changes in lipid peroxidation, blood hematology, biochemical parameters and semen quality of male rats: protective role of vitamin E and β-carotene. *Food and Chemical Toxicology,* 42(10), 1563-1571.

García-Niño, W.R., & Pedraza-Chaverrí, J. (2014). Protective effect of curcumin against heavy metals-induced liver damage. *Food and Chemical Toxicology,* 69, 182-201.

Jacquillet, G., Barbier, O., Cougnon, M.*, et al.* (2006). Zinc protects renal function during cadmium intoxication in the rat. *American Journal of Physiology-Renal Physiology,* 290(1), F127-F137.

Jin, Y., Zhang, S., Tao, R.*, et al.* (2014). Oral exposure of mice to cadmium (II), chromium (VI) and their mixture induce oxidative-and endoplasmic reticulum-stress mediated apoptosis in the livers. *Environmental Toxicology*, 693-705.

Jomova, K., & Valko, M. (2011). Advances in metal-induced oxidative stress and human disease. *Toxicology,* 283(2), 65-87.

Khlifi, R., Olmedo, P., Gil, F.*, et al.* (2013). Arsenic, cadmium, chromium and nickel in cancerous and healthy tissues from patients with head and neck cancer. *Science of the Total Environment,* 452, 58-67.

Kumar, A., & Kumar, A. (2013). Impact of dietary glutathione on hematological indices in rats poisoned with hexavalent chromium. *Journal of Applied and Natural Science,* 5(1), 217-220.

Kumar, A., Rana, S., & Prakash, R. (1984). Dysenzymia induced by hexavalent chromium in rat liver. *International Journal of Tissue Reactions,* 7(4), 333-338.

Kumar, C., Rani, M.U., Reddy, K.K., & Reddy, A.G. (2013). Effect of probiotic strain Lactobacillus casei strain 17 against toxicity induced by chromium in female reproductive system of rats. *International Journal of Pharma and Bio Sciences,* 4(1), 1119-1130.

Lakshmi, G.D., Kumar, P.R., Bharavi, K.*, et al.* (2012). Protective effect of Tribulus terrestris linn on liver and kidney in cadmium intoxicated rats. *Indian Journal of Experimental Biology,* 50, 141-146.

Langárd, S., & Costa, M.A.X. 2007. Chromium. In: Handbook on the Toxicology of Metals Nordberg G.F., Fowler B.A., & Nordberg M., editors. Third Edition ed. Burlington: Academic Press. pp 487-510.

Madejczyk, M.S., Baer, C.E., Dennis, W.E.*, et al.* (2015). Temporal changes in rat liver gene expression after acute cadmium and chromium exposure. *PloS One,* 10(5), e0127327.

Malan, M., Müller, F., Cyster, L., Raitt, L., & Aalbers, J. (2015). Heavy metals in the irrigation water, soils and vegetables in the Philippi horticultural area in the Western Cape Province of South Africa. *Environmental Monitoring and Assessment,* 187(1), 1-8.

Prozialeck, W.C., & Edwards, J.R. (2012). Mechanisms of cadmium-induced proximal tubule injury: new insights with implications for biomonitoring and therapeutic interventions. *Journal of Pharmacology and Experimental Therapeutics,* 343(1), 2-12.

Rana, S., Singh, R., & Verma, S. (1996). Protective effects of few antioxidants on liver function in rats treated with cadmium and mercury. *Indian Journal of Experimental Biology,* 34(2), 177-179.

Reagan-Shaw, S., Nihal, M., & Ahmad, N. (2008). Dose translation from animal to human studies revisited. *The FASEB Journal,* 22(3), 659-661.

Sarkar, A., Ravindran, G., & Krishnamurthy, V. (2013). A brief review on the effect of cadmium toxicity: from cellular to organ level. *International Journal of Bio-Technology and Research,* 3(1), 17-36.

Suzuki, T., Ishihara, K., Migaki, H.*, et al.* (2005). Zinc transporters, ZnT5 and ZnT7, are required for the activation of alkaline phosphatases, zinc-requiring enzymes that are glycosylphosphatidylinositol-anchored to the cytoplasmic membrane. *Journal of Biological Chemistry,* 280(1), 637-643.

Tchounwou, P.B., Yedjou, C.G., Patlolla, A.K., & Sutton, D.J. 2012. Heavy Metal Toxicity and the Environment: Springer.

Thévenod, F., & Lee, W.-K. (2015). Live and let die: roles of autophagy in cadmium nephrotoxicity. *Toxics,* 3(2), 130-151.

Timbrell, J. 1999. Principles of Biochemical Toxicology: CRC Press. 404 p.

Venter, C., & Oberholzer, H.M. 2015. An *in ovo* investigation of the cellular effects of the heavy metals cadmium and chromium alone and in combination. University of Pretoria. Pretoria, South Africa.

Venter, C., Oberholzer, H.M., Taute, H., Cummings, F.R., & Bester, M.J. (2015). An *in ovo* investigation into the hepatotoxicity of cadmium and chromium evaluated with light-and transmission electron microscopy and electron energy-loss spectroscopy. *Journal of Environmental Science and Health. Part A: Toxic/Hazardous Substances & Environmental Engineering,* 50(8), 830-838.

W.H.O. 2011. Guidelines for drinking-water quality World Health Organization. Geneva, Switzerland.